European Journal of Medicinal Chemistry xxx (2016) 1–12

Contents lists available at ScienceDirect

European Journal of Medicinal Chemistry

journal homepage: http://www.elsevier.com/locate/ejmech

Research paper

Affinity-based small fluorescent probe for NAD(P)H:quinone oxidoreductase 1 (NQO1). Design, synthesis and pharmacological evaluation

Jinlei Bian [a, 1], Xiang Li [a, 1], Lili Xu [a], Nan Wang [a], Xue Qian [a], Qidong You [a, *], Xiaojin Zhang [a, b, **]

[a] State Key Laboratory of Natural Medicines and Jiangsu Key Laboratory of Drug Design and Optimization, China Pharmaceutical University, Nanjing, 210009, China
[b] Department of Organic Chemistry, China Pharmaceutical University, Nanjing, 210009, China

ARTICLE INFO

Article history:
Received 18 September 2016
Received in revised form
27 October 2016
Accepted 28 October 2016
Available online xxx

Keywords:
Fluorescent probe
NQO1
Inhibitor
FITC
Dicoumarol

ABSTRACT

NQO1 is a dimeric flavoprotein which intimately associated with cancer and overexpressed in the cytosol of numerous human tumor cells. Given that the cellular environment is quite dynamic and versatile, further investigation of the function of NQO1 depends on tools for specific detection of it. Currently, several activity-based assays have been developed to detect NQO1-expressing cancerous tissues. Herein, we report the development of a functional affinity-based small-molecule probe which is composed of a potent small-molecule NQO1 inhibitor **3d** as the recognition group, a linker and the fluorophores group FITC. The probe exhibits good inhibitory activity of NQO1 and has been successfully used to label the protein in A549 cells at the micromolar level. These features make the probe favorable for mechanistic studies and cancer diagnostic biomarker. Based on these preliminary results, our laboratory will focus on the further development of fluorescent probe for NQO1, which could be anticipated to be applied in physiological and pathological studies of NQO1.

1. Introduction

NAD(P)H:quinone oxidoreductase-1 (NQO1, DT-diaphorase) is a cytosolic flavoenzyme, which is initially identified as a chemo-preventive enzyme and now recognized plays of other biological process including catalyze bioactivation of antitumor quinones and act as chaperone protein, constitute attractive pharmacological targets for development of anticancer therapeutics [1–3]. Indeed NQO1 has been found to be a promising therapeutic target for cancer therapy and several of NQO1 substrates are in multiple clinical trials [4–7]. Considering that the cellular environment is quite dynamic and versatile, the further exploration of function and therapeutic potential of NQO1 under various condition is quite urgent. These achievements depend on the tools for specific and real-time detection of the NQO1 protein.

In the last decade, fluorescence-based techniques have undergone a huge development for studying pharmacological and biochemical processes [8–10]. Given the sensitivity of fluorescence detection and its simplicity, this fluorescent-based methodology appears an important tool in many areas and is being employed for discovery of gene-targeted drugs, molecular biological and protein-protein interaction studies [11,12]. Actually, several activity-based fluorescent probes which can be triggered by NQO1 have been discovered recently (Probe **I** and Probe **II**, Fig. 1A) [13,14]. This type of probes was designed based on NQO1-mediated redox property, thus there are potential possibility for these probes triggered by other quinone oxidoreductases. Therefore, small-molecule fluorescent probe based on binding-signal output principle is needed to be developed. In this work, we reported the first small-molecule fluorescent probe based on affinity which can be used for and

Abbreviations: NQO1, NAD(P)H:quinone oxidoreductase-1; DIC, Dicoumarol; β-lap, β-lapachone; DMSO, Dimethyl sulfoxide; HPLC, High performance liquid chromatography; BSA, Bovine serum albumin; PDB, Protein data bank; equiv, Equivalent; MTT, 3-(4,5-dimethylthiazol-2-yl)-2,5-diphenyltetrazolium bromide; NSCLC, Non-small cell lung cancer; DIC, Dicoumarol; MOE, Molecular operating environment; FITC, Fluorescein isothiocyanate.

* Corresponding author.
** Corresponding author. State Key Laboratory of Natural Medicines and Jiangsu Key Laboratory of Drug Design and Optimization, China Pharmaceutical University, Nanjing, 210009, China.
E-mail addresses: youqd@163.com (Q. You), zxj@cpu.edu.cn (X. Zhang).

[1] These two authors contributed equally to this work.

http://dx.doi.org/10.1016/j.ejmech.2016.10.062
0223-5234/

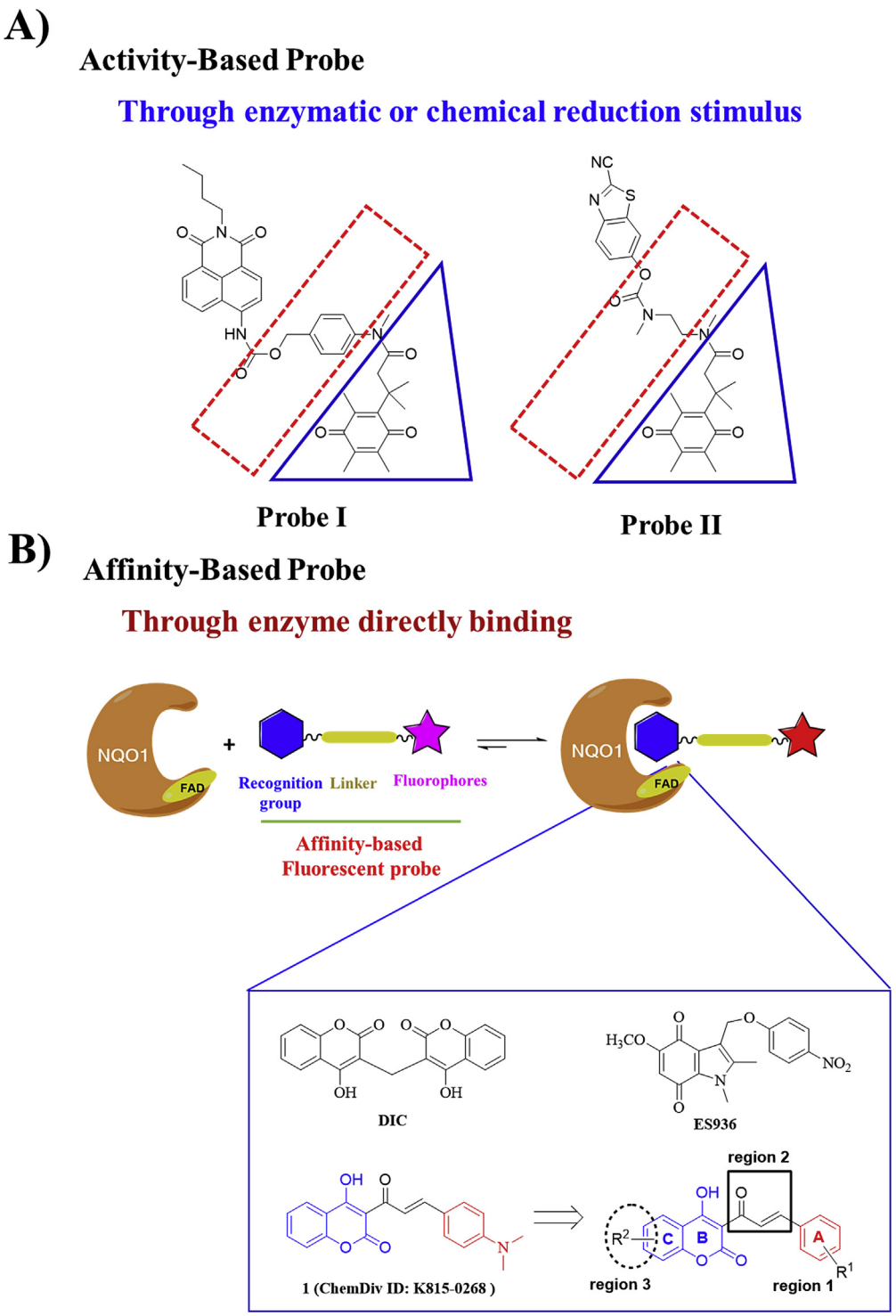

Fig. 1. (A) The structures of activity-based probe. (B) The principle of affinity-based probe and the structures of NQO1 inhibitors (DIC, ES936 and previous reported compound **1**).

fluorescence polarization method and fluorescently visualize and specifically detect NQO1 (Fig. 1B).

To construct a useful probe, it is a pre-requisite to develop a potent and specific inhibitor as the recognition group. A few of compounds are known to inhibit the activity of NQO1 by competing with NAD(P)H for binding to the enzyme [4]. These inhibitors mainly include a series of flavones, coumarins and triazoloacridin-6-ones [15,16]. Among them, dicoumarol (DIC) and ES936 are the most commonly used as a pharmacological inhibitor to study the function of NQO1 in cells (Fig. 1A) [17]. Particularly, it should be emphasized that ES936 is a mechanism-based suicide inhibitor which is different with the competitive inhibitor DIC [13]. Thus, competitive inhibitor DIC is more suitable than ES936 for developing affinity-based fluorescent probe. However, there are still some disadvantages with DIC in that it is not specific towards NQO1 [18]. Therefore, to discover a suitable recognition group for the affinity-based probe, we need to turn our attention to some other competitive inhibitors.

Please cite this article in press as: J. Bian, et al., Affinity-based small fluorescent probe for NAD(P)H:quinone oxidoreductase 1 (NQO1). Design, synthesis and pharmacological evaluation, European Journal of Medicinal Chemistry (2016), http://dx.doi.org/10.1016/j.ejmech.2016.10.062

Recently, we have been focused on discovering NQO1 inhibitors with novel chemical scaffolds [17]. Among these novel NQO1 inhibitors, **1** (ChemDiv ID: K815-0286) showed the most potent inhibitory activity against NQO1. In order to discover more potent inhibitors, a series of compounds were designed based on **1** through rational drug designation. On the basis of more potent inhibitor small-molecule ligand of NQO1, we then reported the design, synthesis, and application of the affinity-based small probe to fluorescently visualize and specifically detect NQO1, which can be applied in further research of NQO1.

2. Result and discussion

2.1. Designation of derivatives of *1*

In order to optimize the structure of **1**, the docked posed of the identified hit was analyzed within the NQO1 binding pocket compared to DIC (Fig. 2). The general molecular orientation and the spatial location of the chemical features of **1** were similar to DIC (PDB ID: 2F1O). It was noted that, based in the docking pose, the side chain was observed that it could occupy the additional pocket formed by Tyr128, Phe232 and some other residues. As our previous work reported, residues that involved most prominent conformation changes that occur in the presence of inhibitors of NQO1 were Tyr128 and Phe232 [17]. Therefore, the fragment A (region 1, Fig. 1B) was a possible modification site, and then the *para*-dimethylaminophenyl was replaced by a series of substituted aromatic ring. Moreover, substituents that can intercalate between and form van der Waals interactions with Trp105 minipocket were also favorable [19]. Thus, we also designed several compounds with substituents at ring C (region 3, Fig. 1B). Representative compounds were also reduced to investigate the role of α,β-unsaturated ketone in inhibiting NQO1 (region 2, Fig. 1B).

2.2. Chemistry

2.2.1. Synthesis of inhibitors

The common synthetic route of compounds **3a-3z** was outlined in Scheme 1. Most of the target compounds (**3a-3v**) were synthesized using 4-hydroxy-2*H*-chromen-2-one (**5**) as the starting material. As for compounds **3w-3z**, the substituted 4-hydroxy-2*H*-chromen-2-ones were preparing by base-mediated cyclization of the corresponding 2-hydroxy acetophenones (**4**) with diethyl carbonate [20]. Compound **6** was prepared by reaction of 4-hydroxycoumarine with $POCl_3$ in the presence of acetic acid. The resulting product **6** was then reacted with aryladehydes to give the target compounds (**3a-3s**, **3w-3z**) in 34–75% yields, which precipitated out from the boiling methanol solution after mixing **6** with corresponding aldehyde. Palladium-carbon catalyzed hydrogenation of the double bond of **3a**, **3d** and **3s** to provide the product **3t-3v** in 35–86% yield. The structures of all compounds were confirmed by ^1H NMR and electrospray ionization mass spectrometry (ESI-MS). Before these compounds were used in biological experiments, they were purified by silica gel column chromatography and HPLC was used to determine their purity (all > 95%).

2.2.2. Synthesis of the fluorescent probe

Starting with 4-hydroxy-3-(3-(4-hydroxyphenyl)acryloyl)-2*H*-chromen-2-one, the probe **III** was synthesized in three steps (Scheme 2). First, aminoalkanols (**7**) with carbon atom spacers of six were Boc-protected to give intermediate **8** in excellent yields (85%). Treatment **8** with tosyl chloride provided the product **9** in 81% yields. The condensation of compound **3d** with **9** under the base of K_2CO_3 affords compound **10** with the linker. By removing the Boc protecting groups, we got the key intermediate **11**. Finally, the probe **III** was obtained through conjugating the fluorescein isothiocyanate (FITC) group with compound **11**.

2.3. Inhibitory activity on recombinant hNQO1 of all compounds

The 26 newly synthesized compounds were evaluated for their ability to inhibit recombinant NQO1 *in vitro*. All of these inhibitors were assayed in the presence of 0.14% (*w*/*v*) bovine serum albumin (BSA), considering the effect of nonspecific protein binding [18,21]. The inhibition rates of these derivatives at 10 μmol L^{-1} were shown in Table 1. These compounds can be divided into three categories (Fig. 1B). To investigate the A-ring substituent effects on the inhibition of NQO1, nineteen compounds (**3a-3s**) with different substituent groups at A-ring were synthesized (region 1). In general, most of these compounds possessed moderate to good inhibition rates of NQO1, indicating that these compounds were potential inhibitors for NQO1. Compounds **3d**, **3e**, **3m**, **3n** and **3s** substituted with electron-donating group (4-OH, 4-NH_2, 2,3-OCH_3, 4-OEt and 3-OCH_3) at A-ring displayed excellent inhibition rates of NQO1 ranging from 81.7% to 92.7%. In addition, the presence of strong electron-withdrawing group at A-ring, such as **3b**, **3g**, **3h** and **3i** substituted with 4-NO_2, 4-CN, 3-NO_2 and 4-CF_3 functional groups, was unfavorable for inhibiting NQO1 activity. With regard to naphthyl substitution (**3q**), the activity decreased sharply. This phenomenon was possibly due to the fact that the binding pocket

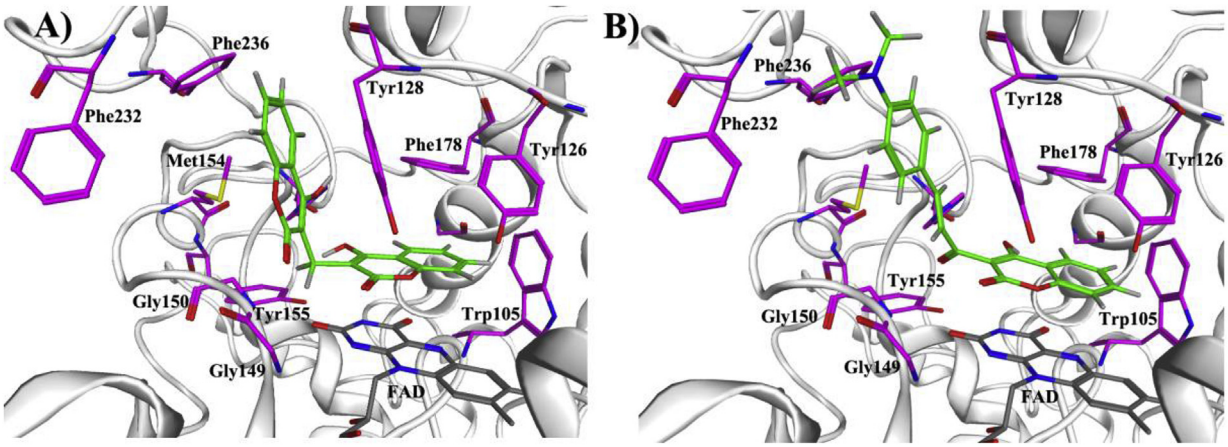

Fig. 2. The crystal binding mode of DIC and docking-predicted binding mode of **1**. (A) DIC and (B) **1** in the active site of NQO1 respectively, key residues were labeled in stick.

Please cite this article in press as: J. Bian, et al., Affinity-based small fluorescent probe for NAD(P)H:quinone oxidoreductase 1 (NQO1). Design, synthesis and pharmacological evaluation, European Journal of Medicinal Chemistry (2016), http://dx.doi.org/10.1016/j.ejmech.2016.10.062

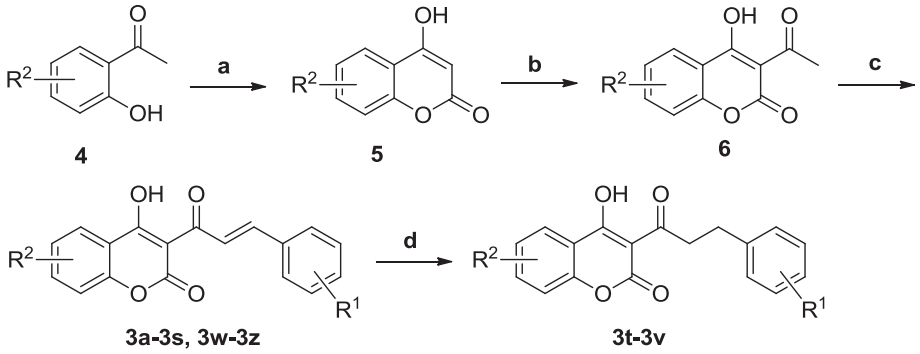

Scheme 1. Reagents and conditions: (a) $(EtO)_2CO$, NaH, 0 °C to r.t., 0.5 h to 100 °C, 2 h, 60–69%; (b) HOAc, $POCl_3$, reflux, 75min, 32–58%; (c) aryladehydes, piperidine, $CHCl_3$, reflux, 3–40 h, 34–75%. (d) H_2, Pd/C, r.t., 10 h, 35–86%.

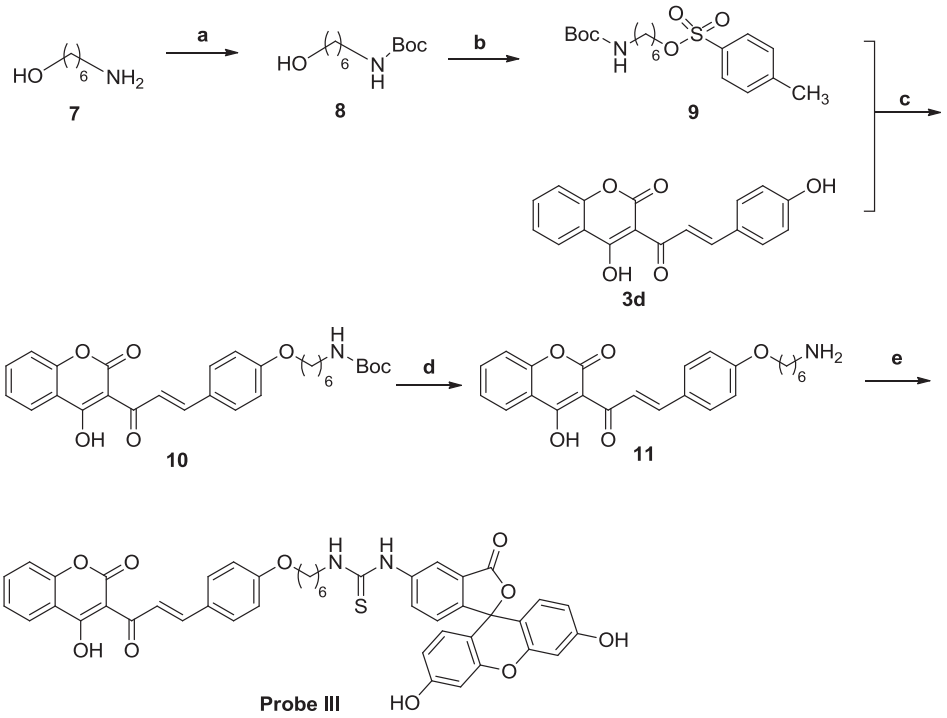

Scheme 2. Reagents and conditions: (a) DCM, r.t., 5min, 85%; (b) Et_3N, DCM, 48 h; (c) K_2CO_3, DMF, 80 °C, 8 h, 15%; (d) CF_3COOH, DCM,, r.t., 20min, 80%; (e) DMF, r.t., 1 h.

was not large enough for naphthyl group binding. Among these A-ring substituted derivatives (**3a-3s**), compound **3a** with *para*-chloro substitution exhibited the most potent inhibition rates of NQO1 (91.1 ± 4.3%) at 10 μM. As for the region 2 investigated compounds **3t-3v**, which were obtained from reducing the double bonds of α,β-unsaturated ketone of compounds **3a**, **3d** and **3s**, the inhibition rates of these compounds were still retained though significantly decreased, demonstrating that the olefinic bond may contribute to the inhibitory activity. Compounds (**3x-3z**) with methyl or methoxy groups at C-ring (region 3) showed equal or slightly better inhibition rates of NQO1 compared to the unsubstituted compounds (**3a** and **3s**), indicating that methyl- or methoxy-substitutions were tolerable for NQO1 inhibitors. However, when chloric substituent was introduced in the C-ring (**3w**), the inhibition rate was dramatically reduced (see Table 2).

Representative compounds **3a**, **3d**, **3x** and **3z** that showed good inhibition activities at the concentration of 10 μM were selected to determine their IC_{50} values. DIC was also evaluated as a comparison group (Fig. 3). All of the compounds revealed the same level inhibitory activity compared to DIC. Notably, compound **3z** was even slightly more potent than the positive control DIC with an IC_{50} of 0.35 ± 0.13 μmol L^{-1}.

2.4. Molecular modeling

For purpose of investigating the binding mechanism of these inhibitors, we then performed molecular docking experiments. All of these compounds (**3a-3z**) were docked into the active site of NQO1 using Gold 5.1 [22,23]. As shown in Table 1, ChemScore values of most derivatives were similar to the control DIC, explained that these derivatives possessed moderate to good inhibition rates of NQO1. Interestingly, according to the docking results, the electronic effects afforded by the additional functional groups at A ring did impact the scores of the derivatives, compounds (**3a**, **3d**, **3m**, **3n**, **3o** and **3s**) with halogen, methoxy or ethoxy substitution at the para position of benzene moiety provided better scores. As for compounds **3t-3v**, their docking scores were lower than other compounds. This could be ascribed to the

Please cite this article in press as: J. Bian, et al., Affinity-based small fluorescent probe for NAD(P)H:quinone oxidoreductase 1 (NQO1). Design, synthesis and pharmacological evaluation, European Journal of Medicinal Chemistry (2016), http://dx.doi.org/10.1016/j.ejmech.2016.10.062

Table 1
Inhibition of hNQO1 by compounds **3a-3z** and DIC.

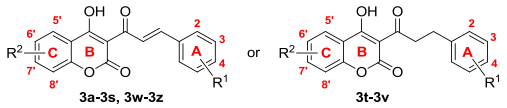

Entry	Cpd	R^1	R^2	NQO1 IR (%) (10 μM) with BSA[a]	Percentage of remaining A549 cells at 50 μM[b]	Chemscore
1	**3a**	4-Cl	H	91.1 ± 4.3	>80	96.46
2	**3b**	4-NO_2	H	71.2 ± 8.1	34 ± 12	92.42
3	**3c**	4-CH_3	H	64.3 ± 3.1	74 ± 11	93.66
4	**3d**	4-OH	H	89.2 ± 11	>80	99.51
5	**3e**	4-NH_2	H	81.7 ± 9.8	>80	91.83
6	**3f**	4-F	H	66.7 ± 5.4	76 ± 13	91.70
7	**3g**	4-CN	H	34.4 ± 6.5	>80	93.17
8	**3h**	3-NO_2	H	65.8 ± 8.7	43 ± 11	91.74
9	**3i**	4-CF_3	H	60.4 ± 3.3	>80	87.64
10	**3j**	2-Cl	H	70.9 ± 10	>80	92.54
11	**3k**	4-iPr	H	51.0 ± 4.9	>80	93.84
12	**3l**	3-Cl	H	54.3 ± 6.5	>80	93.31
13	**3m**	2,3-OCH_3	H	86.9 ± 5.1	>80	96.98
14	**3n**	4-OEt	H	86.7 ± 7.1	>80	94.13
15	**3o**	2,4-Cl	H	87.2 ± 4.5	>80	95.73
16	**3p**	4-Ph	H	79.6 ± 12	>80	89.89
17	**3q**	3,4-C_4H_4	H	46.1 ± 8.1	71 ± 12	88.40
18	**3r**	2-F	H	69.4 ± 4.4	>80	96.44
19	**3s**	3-OCH_3	H	92.7 ± 6.3	>80	95.03
20[b]	**3t**	4-Cl	H	61.4 ± 5.0	>80	93.76
21[b]	**3u**	4-OH	H	77.7 ± 3.9	>80	91.90
22[b]	**3v**	3-OCH_3	H	57.8 ± 8.7	67 ± 23	90.77
23	**3w**	3-OCH_3	6-Cl	74.4 ± 4.0	>80	91.18
24	**3x**	3-OCH_3	6-OCH_3	89.7 ± 3.6	>80	96.23
25	**3y**	3-OCH_3	6,7-CH_3	81.2 ± 3.9	>80	94.31
26	**3z**	4-Cl	6,7-CH_3	99.6 ± 5.1	>80	99.05
27	**DIC**	–	–	81.2 ± 4.8	>80	98.00

[a] The inhibitory ratio of each compound at 10 mM to inhibit purified hNQO1 activity in the presence of 0.14% (w/v) BSA.
[b] The percentage of remaining A549 cells after incubation with compound at 50 μM after 48 h. Most of the derivatives showed non-toxic towards A549 cells and could be employed as useful probe for studying the function of NQO1 in cells.

Table 2
The values of the concentration of selected inhibitors to cause 50% toxicity in A549 cells in the presence of 20 μM β-lap. The results reflected the ability of the inhibitors to inhibit NQO1 activity in A549 cells.

Entry	Cpd	Structure	Concentration required to protect against β-lap toxicity (μM)[a]
1	**3a**	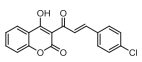	26 ± 3.2
2	**3d**	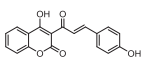	8.4 ± 0.7
3	**3q**	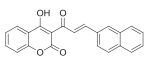	>100
5	**3x**	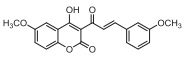	18 ± 3.8
4	**3z**	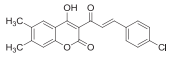	3.6 ± 1.2
6	DIC	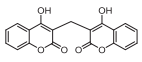	11 ± 1.6

[a] Concentrations of each compounds that causes 50% toxicity in cells in the presence of 20 μM β-lap.

flexible of the conformation by reduction of olefinic bond, which resulted in reduction of inhibitory rates of NQO1. Fig. 4 presented the best-ranked pose of representative compounds **3a** and **3z**. The coumarin ring made π-stacking interaction with the isoalloxazine ring of the bound cofactor FAD, which was similar to the crystal structures of DIC in complex with NQO1 (Fig. 4A and B). In addition, the side chain of these compounds could fit deep into the pocket and make the same π-stacking interactions with Tyr128 and Phe232 in the side binding hydrophobic pocket of NQO1. As for compound **3z**, the two methyls at the C ring can form additional C–H … π interaction with the adjacent Phe178 and Trp105 residues, which was observed for enhancing π-stacking interaction

Please cite this article in press as: J. Bian, et al., Affinity-based small fluorescent probe for NAD(P)H:quinone oxidoreductase 1 (NQO1). Design, synthesis and pharmacological evaluation, European Journal of Medicinal Chemistry (2016), http://dx.doi.org/10.1016/j.ejmech.2016.10.062

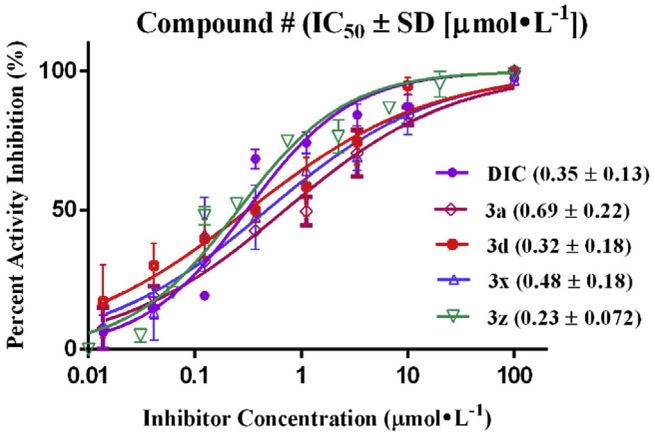

Fig. 3. The IC_{50} curves of DIC and the representative compounds (**3a**, **3d**, **3x** and **3z**).

with surrounding residues, supporting **3z** was the most potent inhibitor of NQO1.

2.5. Evaluation of NQO1 inhibitors in A549 cell lines

In this work, the main goal for discovering NQO1 inhibitors was to develop fluorescent probe for NQO1 as tool to better understand the pharmacological function of NQO1. Hence, compounds with little to no cytotoxic effects are required. A549 (NQO1-rich) cell lines were first treated for 48 h with 50 μmol L^{-1} of these compounds to determine their cytotoxicity. As shown in Table 1, most of the derivatives showed non-toxic towards A549 cells with more than eighty percentage of remaining A549 cells at 50 μM. Hence, these compounds could be promising NQO1 recognition group for further studies.

Moreover, in order to establish the potency and functional ability of the novel series of compounds as inhibitors of NQO1 in cells, A549 cells were then treated with 20 μM β-lapachone (β-lap) and varying concentrations of each representative derivatives (**3a**, **3d**, **3q**, **3x** and **3z**). β-Lap was generally recognized as potential substrates for NQO1 and the ability to modulate β-lap toxicity can be regarded as surrogate measure if the pharmacological efficiency of these compounds to act as inhibitors of NQO1 in cells (Fig. 5A). Among the selected compounds, **3q** was less active than other four compounds according to the results of enzyme assays. 20 μM β-lap alone results in more than 90% reduction in cell proliferation in A549 cells. The concentration of the derivatives needed to inhibit the toxicity of β-lap by 50% can then be used as a measure of the ability of the compounds to inhibit NQO1 in cells. The results of A549 cells exposed to β-lap and the NQO1 inhibitors were shown in Fig. 5B. Except for compound **3q**, which was selected as negative control, other derivatives showed equal potency to DIC to protect against 20 μM β-lap toxicity in A549 cells. In addition, compounds **3d** and **3z** even appeared to be slightly more potent than DIC. The ability of the representative compounds to protect against 20 μM β-lap toxicity in A549 cells was in line with the potency for inhibition of the activity of recombinant NQO1 in the presence of BSA. In addition, **3d** and **3z** were consistently more specific that DIC, suggesting that they could be employed as more pharmacological useful recognition group than DIC for developing fluorescent probe to study the function of NQO1 in cells.

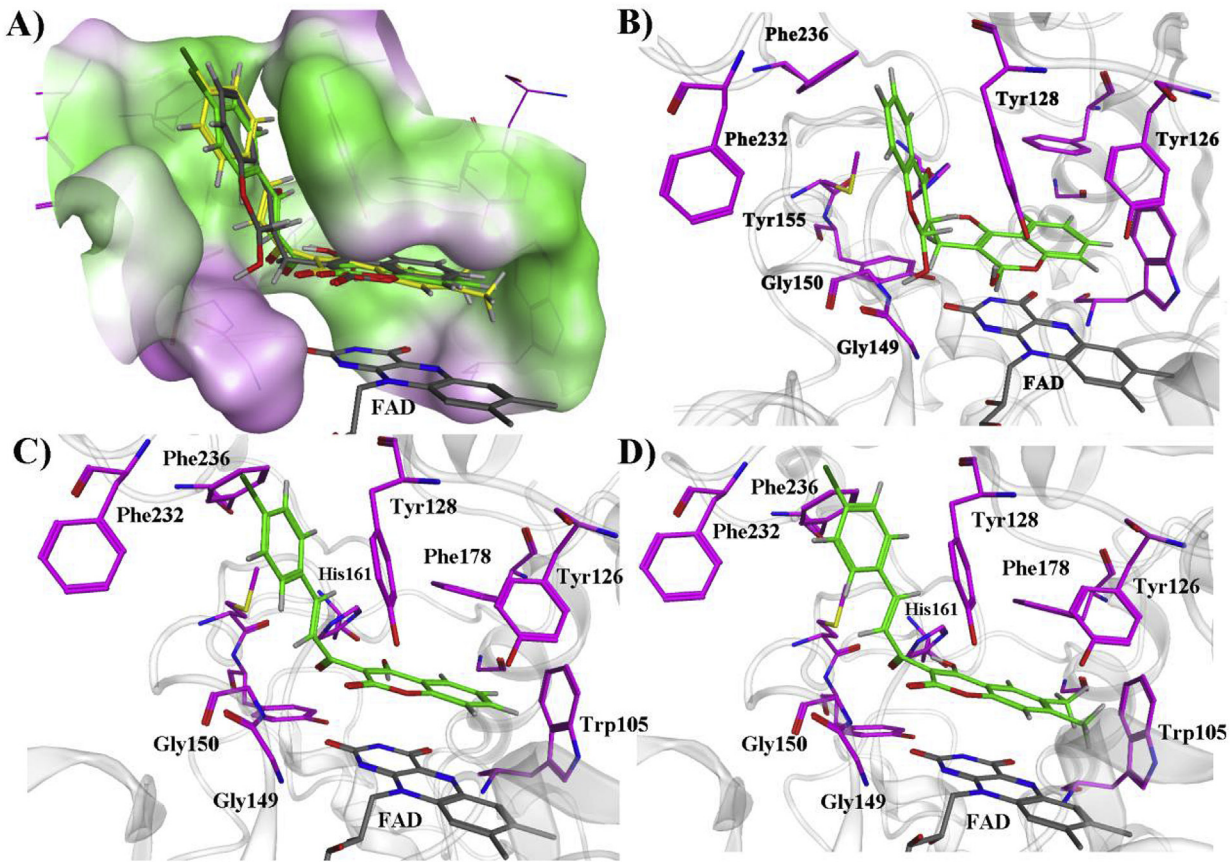

Fig. 4. The crystal binding mode of DIC and docking-predicted binding mode of **3a** and **3z**. (A) the superimposition conformations of DIC, **3a** and **3z** in the active site of NQO1 with a surface colored by lipophilicity state; (B, C, D) DIC, **3a**, **3z** in the active site of NQO1 respectively, key residues were labeled in stick.

Please cite this article in press as: J. Bian, et al., Affinity-based small fluorescent probe for NAD(P)H:quinone oxidoreductase 1 (NQO1). Design, synthesis and pharmacological evaluation, European Journal of Medicinal Chemistry (2016), http://dx.doi.org/10.1016/j.ejmech.2016.10.062

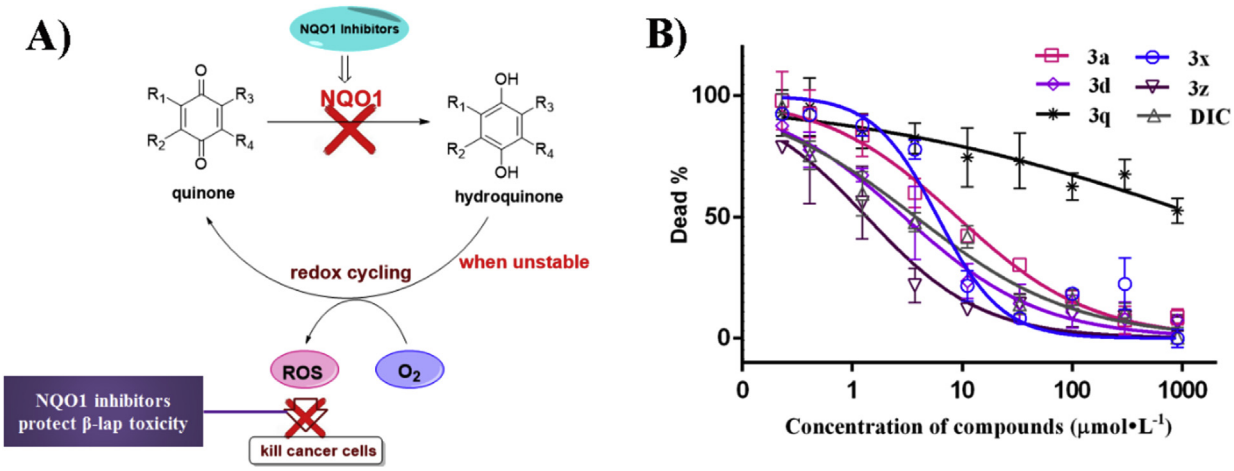

Fig. 5. (A) The role of NQO1 inhibitors was to protect the toxicity of NQO1 substrate (β-lap). (B) A549 cells were treated for 2 h with 20 μM β-lap and varying concentrations of compounds **3a**, **3d**, **3q**, **3x**, **3z** and DIC. The mortality was determined 72 h later by the MTT assay. The concentration of inhibitors to protect 50% toxicity in the presence of 20 μM β-lap was used as the measure of inhibitory potency.

2.6. Design and evaluation of the fluorescent probe

In order to obtain an efficient fluorescent probe, a potent and specific inhibitor was needed. As described above, **3d** and **3z** were the two most efficient inhibitors of NQO1. However, compound **3z** is difficult to obtain, and the deficiency of poor water-soluble also restricted it serve as a tool for further investigation. Therefore, taking both the efficacy and physiochemical property into account, compound **3d** was selected as the recognition group for the probe in the preliminary studies. Subsequently, a new NQO1 fluorescent probe with the general formula was designed on **3d** bearing the fluorescent moiety FITC linked to the *N*-alkyl chain (Fig. 5). Due to the frequently presence of a long-chain alkyl group and FITC in several fluorescent probe, we proposed that the preliminary designed probe might be efficient. The probe was then evaluated for its ability to inhibit recombinant NQO1. The inhibition rate of the probe at 10 μmol L^{-1} was 77% and IC_{50} was 0.98 μM, still in the same range of **3d**, which indicated that the introduction of the FITC group maintained the NQO1 inhibitory activity (Table 3).

2.7. Development of NQO1 fluorescence polarization (FP) assay

As we know, the fluorescence polarization assay is very powerful in measuring real-time protein-inhibitor interactions in solution and quick used for high-throughput drug screening. Hence, we tried to develop the NQO1 fluorescence polarization assay using our obtained fluorescent probe **III**. The principle of fluorescence polarization is according to the observation that when a relatively small, fast-tumbling fluorescent-labeled compound is excited with plane-polarized light, the emitted light is random relative to the plane of polarization, leading to the weak FP response signal (a lower mP value) [24]. When the compound is bound to a bigger molecule such as NQO1, the complex tumbles much slower and the emitted light is polarized, resulting in the enhanced FP response signal (a higher mP value) (Fig. 6A). Therefore, the change of mP reflects the interaction between the fluorescent-labeled compound (in the case probe **III**) and the protein (NQO1). To develop a fluorescence polarization assay, the binding affinity of the probe to the protein should be high and the binding range from maximum mP at saturation to minimal mP at no protein should be large. According to the result, the mP difference value of the probe was about 150, which was in a reasonable range (Fig. 6B). Then, we examined the binding affinity of the probe with NQO1 using FP competition assay. As shown in Fig. 6C, the IC_{50} in the FP assay was 3.14 μM, similar with the method of enzyme activity test (IC_{50} = 0.98 μM), which indicated the effective of the probe.

Table 3
Inhibitory Activity of the recognition group **3d**, the probe III and the control DIC against NQO1.

Cpd	NQO1 IR (%)[a] (10 μM) with BSA	IC_{50} (μM)[b]
DIC	84 ± 4.6	0.37 ± 0.15
3d	86 ± 5.7	0.39 ± 0.10
Probe III	77 ± 6.5	0.98 ± 0.22

[a] The inhibitory ratio of each compound at 10 μM to inhibit purified hNQO1 activity in the presence of 0.14% (w/v) BSA.
[b] The concentration of each compound that inhibits the activity of purified hNQO1 by 50% (IC_{50}).

2.8. Fluorescently visualize cellular NQO1

Because of the good inhibitory activity, probe **III** would be a suitable tool to fluorescently visualize cellular NQO1. In addition, due to NQO1 is expressed in tumor tissue and is absent in normal tissue, NQO1 may be regarded as a potential biomarker for tumors. Accordingly, the imaging of NQO1 could provide useful information for tumor detection and labeling. To highlight this potential, immunofluorescence microscopy was achieved on the tumor cell A549 with high levels of NQO1 expression. The imaging results showed that the probe **III** was able to label NQO1 for visualization (Fig. 7). As a negative control, the inhibition of NQO1 was imaged by incubating the cells with 10 μM DIC together with the probe. Inhibition of NQO1 by DIC resulted in a decrease of fluorescence intensity. The results indicated that probe **III** display favorable selectivity for NQO1 and could be used as a labeling toolkit for NQO1 highly expressing tumor cells.

3. Conclusion

Herein, we reported the details of a study to identify a series of novel NQO1 inhibitors and employed them for the designation of the fluorescent probes. Molecular docking has been applied to analysis the binding modes between the inhibitors and NQO1, and thus to correlate their inhibition rates with predictions of the key

Please cite this article in press as: J. Bian, et al., Affinity-based small fluorescent probe for NAD(P)H:quinone oxidoreductase 1 (NQO1). Design, synthesis and pharmacological evaluation, European Journal of Medicinal Chemistry (2016), http://dx.doi.org/10.1016/j.ejmech.2016.10.062

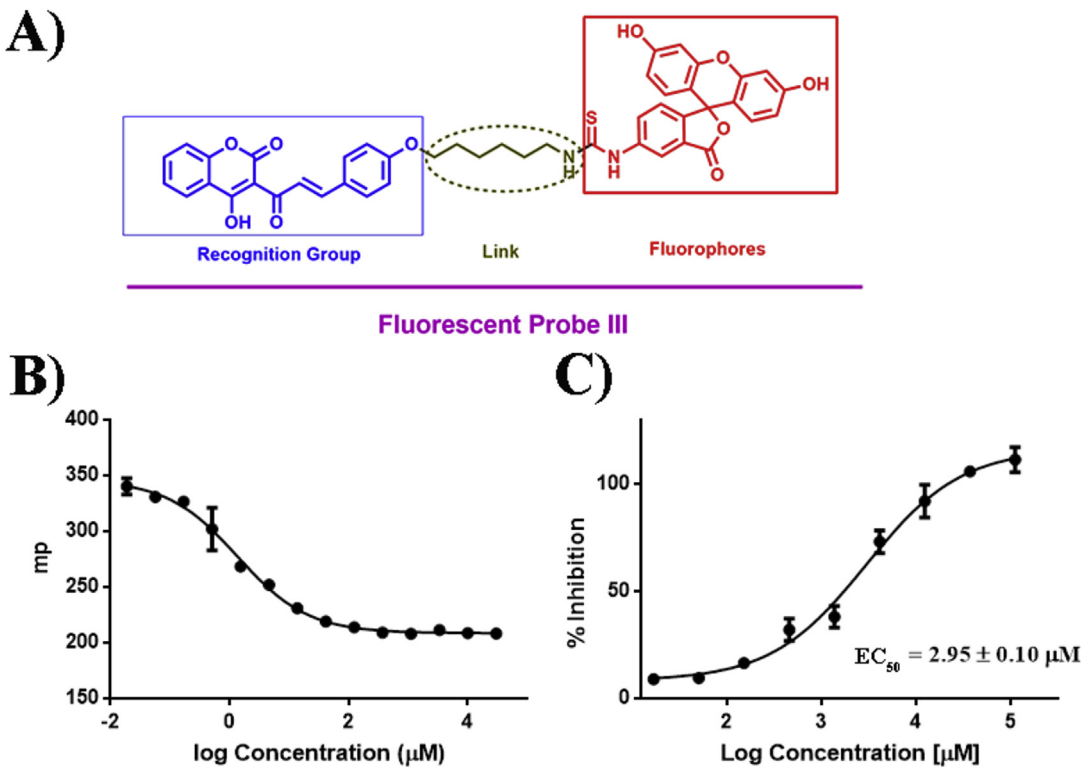

Fig. 6. (A) The structure of probe III. (B) The curve of the probe III. (C) Dose-response inhibition curve of probe III determined by the FP-based binding assay.

interactions in the binding pocket of NQO1. Determination of the ability for protecting against NQO1-mediated toxicity of β-lap confirmed that these inhibitors may be specific for NQO1. In addition, using the potent small-molecule NQO1 ligand **3d** as the structure template, the functional group was attached to the linker afforded the probe with FITC group. The probe exhibited good inhibitory activity of NQO1 and has been successfully used to label the protein in A549 cells at the micromolar level. Furthermore, the preparation of the probe is also convenient. These features make the probe favorable for mechanistic studies and cancer diagnostic biomarker. Based on these preliminary results, our laboratory will focus on the further development of fluorescent probe for NQO1, which could be anticipated to be applied in physiological and pathological studies of NQO1.

4. Experimental

4.1. Chemistry

All reagents were purchased from commercial sources. Organic solutions were concentrated in a rotary evaporator (BüchiRotavapor) below 55 °C under reduced pressure. Reactions were monitored by thin-layer chromatography (TLC) on 0.25 mm silica gel plates (GF254) and visualized under UV light. Melting points were determined with a Melt-Temp II apparatus. The ^{1}H NMR and ^{13}C NMR spectra were measured on a Bruker AV-300 instrument using deuterated solvents with tetramethylsilane (TMS) as internal standard. IR spectra were recorded on a Nicolet iS10 Avatar FT-IR spectrometer using KBr film. EI-MS was collected on shimadzu GCMS-2010 instruments. ESI-mass and high resolution mass spectra (HRMS) were recorded on a Water Q-Tofmicro mass spectrometer. Analytical results are within 0.40% of the theoretical values.

4.1.1. 3-Acetyl-4-hydroxycoumarin (***8***)

To a solution of 4-hydroxy-2*H*-chromen-2-one (3.0 g, 1.86 mmol) in acetic acid (16 mL) was added phosphorus oxychloride (5.6 mL). The mixture was heated at reflux for 75 min. After cooling to room temperature, the precipitate which separated out was collected by filtration and recrystallized from ethanol to give 3-acetyl-4- hydroxy-2*H*-chromen-2-one as light yellow needles (1.66 g, yield 43%). m.p. 134–136 °C. ^{1}H NMR (300 MHz, $CDCl_3$) δ: 17.7 (s, 1H), 7.98 (d, J = 7.9 Hz, 1H), 7.70 (t, J = 7.6 Hz, 1H), 7.37–7.26 (m, 2H), 2.79 (s, 3H). ESI-HRMS m/z $[M+H]^+$ calculated for $C_{11}H_9O_4$: 205.1819, found: 205.1817.

4.1.2. General procedure for the preparation of compounds ***3a-3z***

3-acetyl-4-hydroxy-2*H*-chromen-2-one (0.031 mol) and the substituted aromatic aldehyde (0.03 mol) were dissolved in 30 mL of chloroform. A catalytic amount of piperidine (0.02 mol) was added and the reaction mixture was refluxed till the reaction is finished.

*4.1.2.1. (E)-4-Hydroxy 3-(3-(4-chlorophenyl)acryloyl)-2H-chromen-2-one (**3a**).* Following the procedure above, treatment **6** with 4-chlorobenzaldehyde for 19 h under reflux gave the crude product which recrystallized with methanol to afford **3a** as yellow solid (0.27 g, 75%). m.p. 254–256 °C. ^{1}H NMR (300 MHz, DMSO) δ: 8.27 (d, J = 15.9 Hz, 1H), 8.07 (m, 2H), 8.03 (d, J = 15.7 Hz, 1H), 7.82 (d, J = 5.2 Hz, 2H), 7.58 (d, J = 8.4 Hz, 2H), 7.47–7.43 (m, 2H). ESI-HRMS m/z $[M+H]^+$ calculated for $C_{18}H_{12}ClO_4$: 327.0419, found: 327.0421.

*4.1.2.2. (E)-4-Hydroxy-3-(3-(4-nitrophenyl)acryloyl)-2H-chromen-2-one (**3b**).* Following the procedure above, treatment **6** with 4-nitrobenzaldehyde for 26 h under reflux gave the crude product which recrystallized with ethanol to afford **3b** as yellow solid (0.24 g, 48%). m.p. 197–199 °C. ^{1}H NMR (300 MHz, DMSO) δ: 8.36 (d, J = 15.0 Hz, 1H), 8.34–8.32 (m, 2H), 8.08–8.03 (m, 4H), 8.43 (t,

Please cite this article in press as: J. Bian, et al., Affinity-based small fluorescent probe for NAD(P)H:quinone oxidoreductase 1 (NQO1). Design, synthesis and pharmacological evaluation, European Journal of Medicinal Chemistry (2016), http://dx.doi.org/10.1016/j.ejmech.2016.10.062

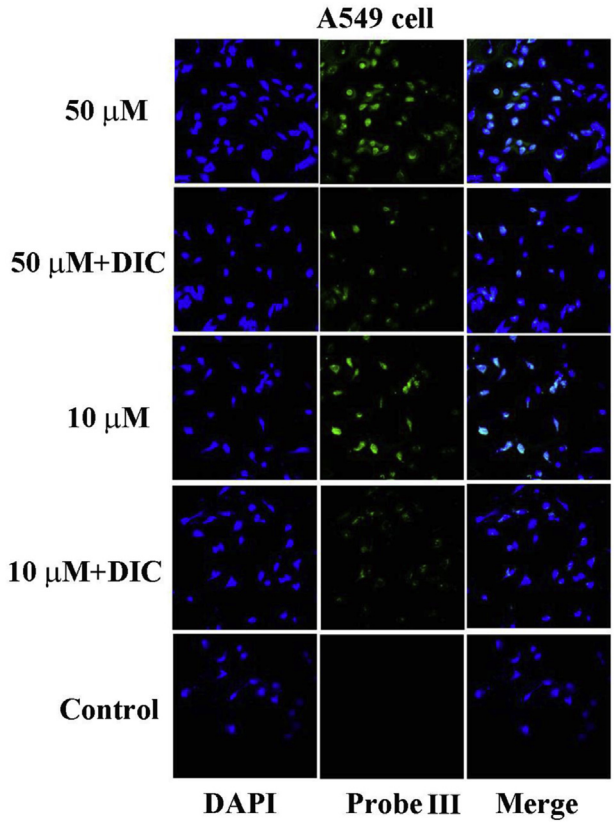

Fig. 7. Fluorescence microscopic imaging of A549 cells incubated with 10 μM or 50 μM probe III. The imaging of inhibition of NQO1 was accomplished by incubating 10 μM DIC with probe. A549 cells were incubated with each probe at 37 °C for 10 min and washed immediately. All images are representative of images obtained in three separate experiments.

J = 7.8 Hz, 1H), 7.47–7.43 (m, 2H). ESI-HRMS m/z $[M-H]^-$ calculated for $C_{18}H_{10}NO_6$: 336.0514, found: 336.0516.

*4.1.2.3. (E)-4-Hydroxy-3-(3-(4-tolyl)acryloyl)-2H-chromen-2-one (**3c**).* Following the procedure above, treatment **6** with 4-methylbenzaldehyde for 18 h under reflux gave the crude product which was purified by column chromatography (eluent: Petroleumether/EtOAc 50:1) to afford the yellow solid **3c** (0.4 g, 40%). m.p. 230–234 °C. ^{1}H NMR (300 MHz, DMSO) δ: 8.26 (d, J = 15.8 Hz, 1H), 8.05 (m, 2H), 8.03 (t, J = 15.7 Hz, 1H), 7.67 (d, J = 7.9 Hz, 2H), 7.45–7.42 (m, 2H), 7.32 (d, J = 7.9 Hz, 2H), 2.35 (s, 3H). ESI-HRMS m/z $[M+H]^+$ calculated for $C_{19}H_{15}O_4$: 308.9080, found: 308.9078. HPLC (90% methanol in water): t_R = 3.391 min, 98.7%. HPLC (90% methanol in water): t_R = 3.246 min, 96.2%.

*4.1.2.4. (E)-4-Hydroxy-3-(3-(4-hydroxyphenyl)acryloyl)-2H-chromen-2-one (**3d**).* Following the procedure above, treatment **6** with 4-hydroxybenzaldehyde for 3 h under reflux gave the orange solid **3d** (0.43 g, 48%). m.p. 244–246 °C. ^{1}H NMR (300 MHz, DMSO) δ: 10.40 (s, 1H), 8.14 (d, J = 4.8 Hz, 1H), 8.01 (m, 2H), 7.79 (t, J = 7.4 Hz, 1H), 7.67 (d, J = 5.1 Hz, 2H), 7.42–7.41 (m, 2H), 6.88 (d, J = 8.6 Hz, 2H). ESI-HRMS m/z $[M+H]^+$ calculated for $C_{18}H_{13}O_5$: 309.0757, found: 309.0762. HPLC (90% methanol in water): t_R = 3.329 min, 98.0%.

*4.1.2.5. (E)-4-Hydroxy-3-(3-(4-aminophenyl)acryloyl)-2H-chromen-2-one (**3e**).* Following the procedure above, treatment **6** with 3-methoxybenzaldehyde for 10.5 h under reflux gave the crude product which recrystallized with ethanol to afford **3e** as yellow solid (0.35 g, 50%). m.p. 235-137 °C. ^{1}H NMR (300 MHz, DMSO) δ: 8.02–7.99 (m, 3H), 7.38–7.45 (m, 2H), 7.52 (d, J = 8.7 Hz, 2H), 7.40–7.37 (m, 2H), 6.65 (d, J = 8.6 Hz, 2H). IR (ν, cm^{-1}): 3416, 1611, 1548, 898. ESI-HRMS m/z $[M+H]^+$ calculated for $C_{18}H_{13}NO_4$: 308.0917, found: 308.0925. HPLC (90% methanol in water): t_R = 3.582 min, 96.3%.

*4.1.2.6. (E)-4-Hydroxy-3-(3-(4-fluorophenyl)acryloyl)-2H-chromen-2-one (**3f**).* Following the procedure above, treatment **6** with 4-fluorobenzaldehyde for 40 h under reflux gave the crude product which was purified by column chromatography (eluent: Petroleumether/EtOAc 5:1) to afford the yellow solid **3f** (0.12 g, 40%). m.p. 197–200 °C. ^{1}H NMR (300 MHz, $CDCl_3$) δ: 8.41 (d, J = 15.6 Hz, 1H), 8.14–8.03 (m, 2H), 7.78–7.70 (m, 3H), 7.40–7.32 (m, 2H), 7.16 (t, J = 17.0 Hz, 2H). ESI-HRMS m/z $[M+H]^+$ calculated for $C_{18}H_{12}FO_4$: 311.0714, found: 311.0710. HPLC (90% methanol in water): t_R = 4.046 min, 98.3%.

*4.1.2.7. (E)-4-Hydroxy-3-(3-(4-cyanophenyl)acryloyl) -2H-chromen-2-one (**3g**).* Following the procedure above, treatment **6** with 4-cyanobenzaldehyde for 26 h under reflux gave the crude product which recrystallized with methanol to afford **3g** as yellow solid (0.32 g, 50%). m.p. 254–256 °C. ^{1}H NMR (300 MHz, DMSO) δ: 8.35 (d, J = 15.8 Hz, 1H), 8.06 (d, J = 7.2 Hz, 2H), 8.00 (s, 4H), 7.85 (d, J = 6.6 Hz, 1H), 7.48–7.45 (m, 2H). ESI-HRMS m/z $[M+H]^+$ calculated for $C_{19}H_{12}NO_4$: 318.3003, found: 318.3005. HPLC (90% methanol in water): t_R = 3.240 min, 96.4%.

*4.1.2.8. (E)-4-Hydroxy-3-(3-(3-nitrophenyl)acryloyl)-2H-chromen-2-one (**3h**).* Following the procedure above, treatment **6** with 3-nitrobenzaldehyde for 26 h under reflux gave the crude product which recrystallized with ethanol to afford **3h** as yellow solid (0.32 g, 64%). m.p. 222–226 °C. ^{1}H NMR (300 MHz, DMSO) δ: 8.59 (s, 1H), 8.39–8.32 (m, 2H), 8.24 (d, J = 7.5 Hz, 1H), 8.58–8.06 (m, 2H), 7.85–7.78 (m, 2H), 7.47 (d, J = 7.5 Hz, 1H). ESI-HRMS m/z $[M+H]^+$ calculated for $C_{18}H_{12}NO_6$: 338.0659, found: 338.0663. HPLC (90% methanol in water): t_R = 3.326 min, 97.2%.

*4.1.2.9. (E)-4-Hydroxy-3-(3-(4-(trifluoromethyl)phenyl)acryloyl)-2H-chromen-2-one (**3i**).* Following the procedure above, treatment **6** with 4-(trifluoromethyl) benzaldehyde for 16.5 h under reflux gave the crude product which was purified by column chromatography (eluent: Petroleumether/EtOAc 30:1) to afford yellow solid **3i** (0.3 g, 34%). m.p. 257–260 °C. ^{1}H NMR (300 MHz, DMSO) δ: 8.36 (d, J = 15.9 Hz, 1H), 8.08–8.03 (m, 2H), 7.99 (d, J = 8.0 Hz, 2H), 7.87 (s, 1H), 7.83 (d, J = 6.8 Hz, 2H), 7.47–7.43 (m, 2H). ESI-HRMS m/z $[M+H]^+$ calculated for $C_{19}H_{12}F_3O_4$: 361.0658, found: 361.3265. HPLC (90% methanol in water): t_R = 3.359 min, 96.8%.

*4.1.2.10. (E)-4-Hydroxy-3-(3-(2-chlorophenyl)acryloyl)-2H-chromen-2-one (**3j**).* Following the procedure above, treatment **6** with 2-chlorobenzaldehyde for 18 h under reflux gave the crude product which was purified by column chromatography (eluent: Petroleumether/EtOAc 10:1) to afford the yellow solid **3j** (0.2 g, 40%). m.p. 270–273 °C. ^{1}H NMR (300 MHz, $CDCl_3$) δ: 8.48 (d, J = 6.1 Hz, 2H), 7.76–7.70 (m, 1H) 7.49–7.46 (m, 1H), 7.40–7.28 (m, 4H). ESI-HRMS m/z $[M+H]^+$ calculated for $C_{18}H_{12}ClO_4$: 327.0419, found: 327.0425. HPLC (90% methanol in water): t_R = 3.489 min, 97.2%.

*4.1.2.11. (E)-4-Hydroxy-3-(3-(4-isopropylphenyl)acryloyl)-2H-chromen-2-one (**3k**).* Following the procedure above, treatment **6** with 4-isopropylbenzaldehyde for 12 h under reflux gave the crude product which was purified by column chromatography (eluent: Petroleumether/EtOAc = 10:1) to afford the yellow solid **3k** (0.36 g,

45%). m.p. 288–290 °C. ^{1}H NMR (300 MHz, DMSO) δ: 8.44 (d, J = 15.6 Hz, 1H), 8.13–8.07 (m, 2H), 7.71–7.68 (m, 3H), 7.38–7.33 (m, 2H), 7.30 (d, J = 9.9 Hz, 2H), 2.98 (m, 1H), 1.28 (d, J = 4.7 Hz, 6H). ESI-HRMS m/z $[M+Na]^+$ calculated for $C_{21}H_{18}NaO_4$: 357.1097, found: 357.1101. HPLC (90% methanol in water): t_R = 3.949 min, 95.9%.

*4.1.2.12. (E)-4-Hydroxy-3-(3-(3-chlorophenyl)acryloyl)-2H-chromen-2-one (**3l**).* Following the procedure above, treatment **6** with 3-chlorobenzaldehyde for 38.5 h under reflux gave the crude product which was purified by column chromatography (eluent: Petroleumether/EtOAc 10:1) to afford the yellow solid **3l** (0.26 g, 45%). m.p. 216–218 °C. ^{1}H NMR (300 MHz, DMSO) δ: 8.30 (d, J = 15.5 Hz, 1H), 8.07–7.97 (m, 2H), 7.78–7.82 (m, 2H), 7.76 (d, J = 7.1 Hz, 1H), 7.57–7.47 (m, 2H), 7.45–7.43 (m, 2H). ESI-HRMS m/z $[M+Na]^+$ calculated for $C_{18}H_{11}NaO_4$: 349.0238, found: 349.0239. HPLC (90% methanol in water): t_R = 3.567 min, 96.4%.

*4.1.2.13. (E)-4-Hydroxy-3-(3-(3,4-dimethoxyphenyl)acryloyl)-2H-chromen-2-one (**3m**).* Following the procedure above, treatment **6** with 3,4-dimethoxybenzaldehyde for 12.5 h under reflux gave the crude product which recrystallized with ethanol to afford **3m** as yellow solid (0.45 g, 75%). m.p. 245–256 °C. ^{1}H NMR (300 MHz, DMSO) δ: 8.03 (d, J = 8.2 Hz, 2H), 7.45 (t, J = 8.1 Hz, 2H), 7.48–7.43 (m, 4H), 7.13 (s, 1H), 2.67 (s, 6H). ESI-HRMS m/z $[M+H]^+$ calculated for $C_{20}H_{17}O_6$: 353.102, found: 353.1018. HPLC (90% methanol in water): t_R = 3.336 min, 97.7%.

*4.1.2.14. (E)-4-Hydroxy-3-(3-(4-ethoxyphenyl)acryloyl)-2H-chromen-2-one (**3n**).* Following the procedure above, treatment **6** with 4-ethoxybenzaldehyde for 7 h under reflux gave the crude product which recrystallized with ethanol to afford **3n** as yellow solid (0.4 g, 40%). m.p. 287–289 °C. ^{1}H NMR (300 MHz, DMSO) δ: 8.30 (d, J = 15.5 Hz, 1H), 8.05–8.03 (m, 2H), 7.83 (m, 1H), 7.75 (d, J = 6.0 Hz, 2H), 7.44 (s, 2H), 7.05 (d, J = 6.5 Hz, 2H), 4.10 (m, 2H), 1.34 (t, J = 6.6 Hz, 3H). ESI-HRMS m/z $[M+Na]^+$ calculated for $C_{20}H_{16}NaO_5$: 359.0890, found: 359.0896. HPLC (90% methanol in water): t_R = 3.736 min, 98.5%.

*4.1.2.15. (E)-4-Hydroxy-3-(3-(2,4-dichlorophenyl)acryloyl)-2H-chromen-2-one (**3o**).* Following the procedure above, treatment **6** with 2,4-dichlorobenzaldehyde for 13 h under reflux gave the crude product which recrystallized with ethanol to afford **3o** as yellow solid (0.3 g, 34%). m.p. 195–198 °C. ^{1}H NMR (300 MHz, DMSO) δ: 8.30 (d, J = 15.7 Hz, 1H), 8.16 (s, 1H), 8.08 (t, J = 7.9 Hz, 1H), 7.93 (d, J = 8.6 Hz, 1H), 7.84–7.81 (m, 2H), 7.50 (d, J = 7.9 Hz, 1H), 7.46–7.43 (m, 2H). ESI-HRMS m/z $[M+H]^+$ calculated for $C_{18}H_{11}Cl_2O_4$: 361.0029, found: 361.0028. HPLC (90% methanol in water): t_R = 3.925 min, 98.0%.

*4.1.2.16. (E)-4-Hydroxy-3-(3-([1,1'-biphenyl]-4-yl)acryloyl)-2H-chromen-2-one (**3p**).* Following the procedure above, treatment **6** with [1,1'-biphenyl]-4-carbaldehyde for 13 h under reflux gave the crude product which recrystallized with ethanol to afford **3p** as yellow solid (0.45 g, 51%). m.p. 200–203 °C. ^{1}H NMR (300 MHz, DMSO) δ: 8.32 (m, 2H), 8.12–8.05 (m, 2H), 7.91–7.84 (m, 4H), 7.76 (d, J = 7.3 Hz, 2H), 7.54–7.43 (m, 5H). ESI-HRMS m/z $[M+H]^+$ calculated for $C_{24}H_{17}O_4$: 369.1121, found: 369.1123. HPLC (90% methanol in water): t_R = 4.096 min, 97.7%.

*4.1.2.17. (E)-4-Hydroxy-3-(3-(naphthalen-2-yl)acryloyl)-2H-chromen-2-one (**3q**).* Following the procedure above, treatment **6** with 2-naphthaldehyde for 11.5 h under reflux gave the crude product which recrystallized with ethanol to afford **3q** as yellow solid (0.5 g, 61%). m.p. 215–217 °C. ^{1}H NMR (300 MHz, DMSO) δ: 8.04 (t, J = 14.9 Hz, 2H), 8.20 (d, J = 15.5 Hz, 1H), 8.08–7.96 (m, 4H), 7.09–7.85 (m, 2H), 7.61 (s, 2H), 7.46 (d, J = 8.2 Hz, 2H). ESI-HRMS m/z $[M+H]^+$ calculated for $C_{22}H_{15}O_4$: 343.0965, found: 343.0965. HPLC (90% methanol in water): t_R = 3.314 min, 94.0%.

*4.1.2.18. (E)-4-Hydroxy-3-(3-(2-fluorophenyl)acryloyl)-2H-chromen-2-one (**3r**).* Following the procedure above, treatment **6** with 2-fluorobenzaldehyde for 18 h under reflux gave the crude product which was purified by column chromatography (eluent: Petroleumether/EtOAc 10:1) to afford the yellow solid **3r** (0.4 g, 64%). m.p. 235–237 °C. ^{1}H NMR (300 MHz, DMSO) δ: 8.40 (d, J = 15.9 Hz, 1H), 8.06–8.01 (m, 2H), 7.85 (m, 2H), 7.60–7.50 (m, 1H), 7.47–7.36 (m, 4H). ESI-HRMS m/z $[M+H]^+$ calculated for $C_{18}H_{12}O_4$: 311.0714, found: 311.0716. HPLC (90% methanol in water): t_R = 10.292 min, 96.4%.

*4.1.2.19. (E)-4-Hydroxy-3-(3-(3-methoxyphenyl)acryloyl)-2H-chromen-2-one (**3s**).* Following the procedure above, treatment **6** with 3-methoxybenzaldehyde for 10.5 h under reflux gave the crude product which recrystallized with ethanol to afford **3s** as yellow solid (0.35 g, 50%). m.p. 267–269 °C. ^{1}H NMR (300 MHz, DMSO) δ: 8.29 (d, J = 13.3 Hz, 1H), 8.05–7.99 (m, 2H), 7.85 (t, J = 6.0 Hz, 1H), 7.44–7.32 (m, 5H), 7.10 (d, J = 6.0 Hz, 1H), 3.82 (s, 3H). ESI-HRMS m/z $[M+H]^+$ calculated for $C_{19}H_{15}O_5$: 323.0915, found: 323.0907. HPLC (90% methanol in water): t_R = 3.460 min, 96.0%.

*4.1.2.20. 4-Hydroxy-3-(3-(4-chlorophenyl)propanoyl)-2H-chromen-2-one (**3t**).* As yellow solid (55% yield). m.p. 132–134 °C. ^{1}H NMR (300 MHz, DMSO) δ: 8.04–8.01 (m, 1H), 7.85–7.81 (m, 1H), 7.46–7.42 (m, 2H), 7.36–7.27 (m, 4H), 3.41 (t, J = 7.5 Hz, 2H), 2.92 (t, J = 7.5 Hz, 2H). IR (ν, cm^{-1}): 3415, 1719, 1618, 991. ESI-HRMS m/z $[M-H]^-$ calculated for $C_{18}H_{12}ClO_4$ 327.0424, found 327.0421. HPLC (90% methanol in water): t_R = 9.717 min, 98.9%.

*4.1.2.21. 4-Hydroxy-3-(3-(4-hydroxyphenyl)propanoyl)-2H-chromen-2-one (**3u**).* As yellow solid (63% yield). m.p. 170–173 °C. ^{1}H NMR (300 MHz, DMSO) δ: 11.75 (s, 1H), 9.20 (s, 1H), 8.04 (dd, J_1 = 8.2 Hz, J_2 = 1.5 Hz, 1H), 7.87–7.81 (m, 1H), 7.48–7.43 (m, 2H), 7.06 (d, J = 8.4 Hz, 2H), 6.68 (d, J = 8.4 Hz, 2H), 3.80–3.75 (m, 2H), 2.82 (t, J = 7.2 Hz, 2H). IR (ν, cm^{-1}): 3415, 1733, 1612, 979. ESI-HRMS m/z $[M-H]^-$ calculated for $C_{18}H_{13}O_5$ 309.0763, found 309.0722. HPLC (90% methanol in water): t_R = 3.061 min, 98.2%.

*4.1.2.22. 4-Hydroxy-3-(3-(3-methoxyphenyl) propanoyl)-2H-chromen-2-one (**3v**).* As orange solid (65% yield). m.p. 110–112 °C. ^{1}H NMR (300 MHz, DMSO) δ: 8.06 (dd, J_1 = 8.2 Hz, J_2 = 1.5 Hz, 1H), 7.88–7.83 (m, 1H) 7.49–7.45 (m, 2H), 7.23 (t, J = 8.1 Hz, 1H), 6.87–6.85 (m, 2H), 6.80–6.76 (m, 1H). IR (ν, cm^{-1}): 3412, 1722, 1606, 902. ESI-HRMS m/z $[M-H]^-$ calculated for $C_{19}H_{15}O_5$ 323.0919, found 323.0947. HPLC (90% methanol in water): t_R = 3419 min, 96.6%.

*4.1.2.23. (E)-3-(3-(4-chlorophenyl)acryloyl)-4-hydroxy-6,7-dimethyl-2H-chromen-2-one (**3w**).* As yellow solid (42% yield). m.p. 236–238 °C. ^{1}H NMR (300 MHz, DMSO) δ: 8.22 (d, J = 16.1 Hz, 1H), 7.92 (d, J = 15.9 Hz, 1H), 7.78–7.75 (m, 3H), 7.55 (d, J = 8.6 Hz, 2H), 7.23 (s, 1H), 2.35 (s, 3H), 2.30 (s, 3H). IR (ν, cm^{-1}): 3412, 1722, 1606, 902. ESI-HRMS m/z $[M-H]^-$ calculated for $C_{20}H_{14}ClO_4$ 353.0581, found 531.0677. HPLC (90% methanol in water): t_R = 5.009 min, 97.7%.

*4.1.2.24. (E)-3-(3-(3-methoxyphenyl)acryloyl)-4-hydroxy-6,7-dimethyl-2H-chromen-2-one (**3x**).* As yellow solid (41% yield). m.p. 197–199 °C. ^{1}H NMR (300 MHz, DMSO) δ: 8.27 (d, J = 15.9 Hz, 1H), 8.27 (d, J = 16.1 Hz, 1H), 7.77 (s, 1H), 7.45–7.34 (m, 2H), 7.28 (d, J = 7.2 Hz, 2H), 7.09 (d, J = 8.3 Hz, 1H), 3.81 (s, 3H), 2.36 (s, 3H), 2.30

Please cite this article in press as: J. Bian, et al., Affinity-based small fluorescent probe for NAD(P)H:quinone oxidoreductase 1 (NQO1). Design, synthesis and pharmacological evaluation, European Journal of Medicinal Chemistry (2016), http://dx.doi.org/10.1016/j.ejmech.2016.10.062

(s, 3H). IR (ν, cm^{-1}): 3414, 1718, 1621, 987. ESI-HRMS m/z $[M+H]^+$ calculated for $C_{21}H_{18}O_5$ 351.1232, found 351.0676. HPLC (90% methanol in water): $t_R = 4.421$ min, 95.3%.

*4.1.2.25. (E)-3-(3-(3-methoxyphenyl)acryloyl)-4-hydroxy-7-chloro-2H-chromen-2-one (**3y**).* As yellow solid (39% yield). m.p. 182–184 °C. ^{1}H NMR (300 MHz, DMSO) δ: 8.24 (d, $J = 16.0$ Hz, 1H), 8.06 (s, 1H), 8.01 (d, $J = 2.4$ Hz, 1H), 7.88 (dd, $J_1 = 9.0$ Hz, $J_2 = 2.3$ Hz, 1H), 7.53–7.41 (m, 3H), 7.33 (s, 1H), 7.14–7.11 (m, 1H), 3.84 (s, 3H). IR (ν, cm^{-1}): 3415, 1718, 1622, 977. ESI-HRMS m/z $[M-H]^-$ calculated for $C_{19}H_{12}ClO_5$ 355.0373, found 355.0365. HPLC (90% methanol in water): $t_R = 3.733$ min, 96.9%.

*4.1.2.26. (E)-3-(3-(3-methoxyphenyl)acryloyl)-4-hydroxy-7-methoxy-2H-chromen-2-one (**3z**).* As yellow solid (50% yield). m.p. 206–208 °C. ^{1}H NMR (300 MHz, DMSO) δ: 9.05 (s, 1H), 6.67 (d, $J = 15.7$ Hz, 1H), 6.23–6.14 (m, 2H), 5.54–5.52 (m, 2H), 5.45 (s, 1H), 5.20 (s, 1H), 5.14–5.08 (m, 2H), 2.11 (s, 3H), 2.03 (s, 3H). IR (ν, cm^{-1}): 3412, 1717, 1618, 857. ESI-HRMS m/z $[M-H]^-$ calculated for $C_{20}H_{15}O_6$ 351.0869, found 351.0697. HPLC (90% methanol in water): $t_R = 3.880$ min, 97.7%.

*4.1.3. N-Boc-6-aminohexan-1-ol (**8**)*

Compound **7** (2.4 g, 1 equ.) was dissolved in CH_2Cl_2 (10 mL), then Boc_2O (5.12 mL, 1.1 equ) was added drop wise under continuous stirring condition and resulting solution was stirred at room temperature for another 10 min. After completion of the reaction (monitored by TLC) the excess solvent was removed under reduced pressure. Added a few PE to obtain white product **8** (3.87, 85%). m.p. 46–48 °C. ^{1}H NMR (300 MHz, $CDCl_3$) δ: 4.50 (brs, 1H), 3.64 (t, $J = 6.5$ Hz, 2H), 3.12 (t, $J = 6.5$ Hz, 2H), 1.57–1.46 (m, 6H), 1.44 (s, 9H).

*4.1.4. 6-((Tert-butoxycarbonyl)amino)hexyl-4-methylbenzenesulfonate (**9**)*

Compound **8** (2.0 g, 1 equ.) was dissolved in CH_2Cl_2, para-toluensulfonyl chloride (2.1 g, 1.1 equ.) in CH_2Cl_2 was added drop wise into the solution. Then trimethylamine was added and the reaction was stirred for another 48 h. After that, poured the solution into water and washed with NaCl, dried by Na_2SO_4, the solvent was removed under reduced pressure. The mixture was further purified using silica gel column chromatography using 5–10% petroleum ether to ethylacetate gradient solvent system to afford the desired pure product with colorless oily matter **9** (1.02, 29%). m.p. 66–68 °C. ^{1}H NMR (300 MHz, $CDCl_3$) δ: 7.77 (d, $J = 8.3$ Hz, 2H), 7.34 (d, $J = 8.0$ Hz, 2H), 4.00 (t, $J = 6.5$ Hz, 2H), 3.05 (brs, 2H), 2.44 (s, 3H), 2.04 (s, 1H), 1.42 (s, 9H), 1.34–1.22 (m, 6H).

*4.1.5. (E)- tert-butyl- (6-(4-(3-(4-hydroxy-2-oxo-2H-chromen-3-yl)-3-oxoprop-1-en-1-yl)ph-enoxy)hexyl)carbamate (**10**)*

To a stirred solution of **3d** (0.68 g, 1 equ.), K_2CO_3 (0.343 g, 1.1 equ.) in DMF (20 mL) under N_2 atmosphere was added **9** (0.83 g, 1 equ.) in DMF. The mixture was then heated at 80 °C for 8 h. The excess solvent was then removed under reduced pressure and the obtained residue was washed successively with water and brine, and extracted with ethylacetate (3 × 10 mL). The organic layer was dried over anhydrous Na_2SO_4 and concentrated under reduced pressure. The crude was recrystallized using ethanol to obtain the pure yellow solid **10** (0.35 g, 15%). m.p. 278–280 °C. ^{1}H NMR (300 MHz, DMSO) δ: 7.88 (dd, $J_1 = 7.7$ Hz, $J_2 = 1.5$ Hz, 1H), 7.64 (d, $J = 15.8$ Hz, 1H), 7.52–7.49 (m, 2H), 7.28 (d, $J = 15.7$ Hz, 1H), 7.18–7.10 (m, 2H), 6.94 (d, $J = 8.7$ Hz, 2H), 6.81–6.79 (m, 1H), 3.98 (t, $J = 6.4$ Hz, 2H), 2.91–2.87 (m, 2H), 1.72–1.68 (m, 2H), 1.36 (s, 9H), 1.30–1.22 (m, 6H).

*4.1.6. (E)-3-(3-(4-((6-aminohexyl)oxy)phenyl)acryloyl)-4-hydroxy-2H-chromen-2-one (**11**)*

To a stirred solution of **11** (0.35 g) in CH_2Cl_2 was added a mixture of CH_2Cl_2/CF_3COOH (1: 1, 10 mL). The mixture was stirred at room temperature for 20 min. After completion of the reaction, the pH was adjusted to 12 using sodium hydroxide solution. Then the precipitate was filtered to obtain the yellow solid **11** (0.23 g, 80%).

*4.1.6.1. (E)-1-(3′,6′-dihydroxy-3-oxo-3H-spiro[isobenzofuran-1,9′-xanthen]-6-yl)-3-(6-(4-(3-(4-hydroxy-2-oxo-2H-chromen-3-yl)-3-oxoprop-1-en-1-yl)phenoxy)hexyl)thiourea (probe **III**).* To a solution of compound **11** (1.0 equ.) in DMF was added FITC (10 equ.). The reaction mixture was stirred at 60 °C for 8 h under nitrogen. The crude product was then diluted in 20 mL of diethyl ether and stirred for 30 min. Then the solution was filtered and the residue was purified by column chromatography on silica gel (eluent: 15% CH_3OH in CH_2Cl_2), resulting in probe **III** as an orange solid (255 mg, 40%). m.p. 286–288 °C. ^{1}H NMR (300 MHz, DMSO) δ: 10.78 (s, 1H), 10.32–10.23 (m, 2H), 8.64 (brs, 1H), 8.41 (s, 1H), 7.93–7.80 (m, 2H), 7.55–7.48 (m, 4H), 7.21–7.13 (m, 3H), 6.98–6.96 (m, 2H), 6.98 (s, 2H), 6.57–6.56 (m, 4H), 4.01 (s, 2H), 3.47 (s, 2H), 2.87 (s, 1H), 2.70 (s, 1H), 1.73 (brs, 2H), 1.57 (brs, 2H), 1.42 (brs, 4H). IR (ν, cm^{-1}): 3414, 1727, 1601, 1385, 1172, 1112, 830, 764, 601, 482. ESI m/z $[M+H]^+$ 797.3.

4.2. Biology

4.2.1. NQO1 inhibition studies

All of the synthesized compounds were assayed for their ability affinities to NQO1 protein, we performed the assay using the methods as previous reported [14]. Briefly, NQO1 was diluted in 50 mmol L^{-1} phosphate buffer to give an enzyme activity that would result in a change in optical absorbance of NQO1 substrate (β-lap) of approximately 0.1 per minute. The enzyme reaction was started by adding 5 mL of this solution to 495 mL of 50 mmol L^{-1} phosphate buffer at pH 7.4 containing 200 mmol L^{-1} NADPH for NQO1, with 0.14% (w/v) BSA, together with various concentrations of the potential inhibitor dissolved in DMSO (final concentration 1.0% v/v). The DMSO concentration used was sufficiently small to ensure minimal perturbation of hydrogen bonding networks in aqueous NQO1 complexes. Reaction was initiated by automated dispensing of the NADPH solution into the wells, and data was recorded at 2 s intervals for 5 min at room temperature (22–25 °C). The oxidation of NADPH to $NADP^+$ was monitored at 340 nm on a Varioskan Flash (Thermo, Waltham, MA). Each measurement was made in triplicate and the experiments carried out three times. The IC_{50} curves were generated using Graphpad Prism 6.

4.2.2. Evaluation of NQO1 inhibitors in A549 cell lines

Representative compounds were selected for their evaluation of in A549 cell lines. Impact of NQO1 inhibition on b-lap toxicity was determined by the MTT assay. Cells were plated in 96-well plates at a density of 10 000 cells per mL and allowed to attach overnight (16 h). Cells were then given 30 μmol L^{-1} DIC or the other compounds with various concentrations of β-lap for 2 h, removed, and replaced with fresh medium and the plates were incubated at 37 °C under a humidied atmosphere containing 5% CO_2 for 72 h. MTT was added and the cells were incubated for another 4 h. Medium/MTT solutions were removed carefully by aspiration, the MTT formazan crystals were dissolved in 100 mL of DMSO, and absorbance was determined on a plate at 540 nm. Values of IC_{50} were calculated as the concentration of β-lap, which in the presence of 30 mmol L^{-1} inhibitors, cause 50% cell kill. All toxicity experiments were repeated on at least three technical replicates. Data were analyzed and curves were generated using Graphpad Prism 6.

Please cite this article in press as: J. Bian, et al., Affinity-based small fluorescent probe for NAD(P)H:quinone oxidoreductase 1 (NQO1). Design, synthesis and pharmacological evaluation, European Journal of Medicinal Chemistry (2016), http://dx.doi.org/10.1016/j.ejmech.2016.10.062

4.2.3. Fluorescence polarization competition assay

The fluorescence polarization (FP) assay was performed on a SpectraMax multi-mode microplate reader (Molecular Devices) using the excitation and emission filters. The plates used for the FP measurements were the black nonbinding surface Corning 3676 384-well plates loaded with 40 μL of assay solution per well, consisting 20 μL various concentrations Probe III and 20 μL HEPES buffer to measure the mP value of the Probe III. As for the determination of the inhibition ability of the Probe III of NQO1, the plates loaded woth 40 μL of assay solution per well, consisting 20 μL HEPES buffer, 10 μL Probe III at varying concentrations, and 10 μL 100 nM NQO1. For fluorescein, 485 nm excitation and 535 nm emission filters were used. The IC_{50} of the Probe III was determined from the plot %inhibition against inhibitor concentration analyzed by Origin 8.5 software.

4.2.4. Fluorescence microscopy imaging

The fluorescent imaging was performed on A549 cells. After the culture medium was removed from the confocal dishes, cells were washed with the corresponding culture medium without fetal bovine serum. Probe III was dissolved in DMSO as a stock solution (10 mM), which was further dilute with corresponding culture medium without fetal bovine serum. Subsequently, Probe III (10 μM or 50 μM) was incubated with A549 cells for 10 min, and then cells were washed with the corresponding culture medium without fetal bovine serum. Cells were then stained with fluorochrome dye DAPI (Santa Cruz biotechnology, Santa Cruz, CA) to visualize the nuclei and observed under a laser scanning confocal microscope (Olympus Fluoview FV1000, Japan).

The imaging of A549 cells was also performed by co-incubation with inhibitor (10 μM DIC) incubation together with the probe (10 μM or 50 μM) at the same conditions, using A549 cells.

Acknowledgements

We are thankful for the financial support of the National Natural Science Foundation of China (No. 81302636, 81603025, 81230078, 81573346), the Natural Science Foundation of Jiangsu Province (No. BK20130656), the National Major Science and Technology Project of China (No. 2013ZX09402102-001-005, 2014ZX09507002-005-015), Specialized Research Fund for the Doctoral Program of Higher Education (No. 20130096110002), the Priority Academic Program Development of Jiangsu Higher Education Institutions (PAPD), and the Project Program of State Key Laboratory of Natural Medicines,China Pharmaceutical University (No. SKLNMZZCX201611).

Appendix A. Supplementary data

Supplementary data related to this article can be found at http://dx.doi.org/10.1016/j.ejmech.2016.10.062.

References

[1] S.L. Winski, M. Faig, M.A. Bianchet, D. Siegel, E. Swann, K. Fung, M.W. Duncan, C.J. Moody, L.M. Amzel, D. Ross, Characterization of a mechanism-based inhibitor of NAD(P)H:quinone oxidoreductase 1 by biochemical, X-ray crystallographic, and mass spectrometric approaches, Biochemistry 40 (2001) 15135–15142.

[2] G.L. David, I. Romieu, J.J. Sienra-Monge, Nicotinamide adenine dinucleotide (phosphate) reduced: quinone oxidoreductase and glutathione S-transferase M1 polymorphisms and childhood asthma, Am. J. Respir. Crit. Care. Med. 168 (2003) 1199–1204.

[3] G. Asher, N. Reuven, Y. Shaul, 20S proteasomes and protein degradation "by default", Bioessays 28 (2006) 844–849.

[4] M.A. Colucci, C.J. Moody, G.D. Couch, Natural and synthetic quinones and their reduction by the quinone reductase enzyme NQO1: from synthetic organic chemistry to compounds with anticancer potential, Org. Biomol. Chem. 6 (2008) 637–656.

[5] D. Kostrzewa-Nowak, M.J. Paine, A. Korytowska, K. Serwatka, S. Piotrowska, C.R. Wolf, J. Tarasiuk, Bioreductive activation of mitoxantrone by NADPH cytochrome P450 reductase. Implications for increasing its ability to inhibit the growth of sensitive and multidrug resistant leukaemia HL60 cell, Cancer Lett. 245 (2007) 252–262.

[6] E.A. Bey, M.S. Bentle, K.E. Reinicke, Y. Dong, C.R. Yang, Girard, An NQO1 and PARP-1-mediated cell death pathway induced in non-small-cell lung cancer cells by β-lap, Proc. Natl. Acad. Sci. U. S. A. 104 (2007) 11832–11837.

[7] J. Bian, B. Deng, L. Xu, X. Xu, N. Wang, T. Hu, Z. Yao, J. Du, L. Yang, H. Sun, X. Zhang, Q. You, 2-Substituted 3-methylnaphtho[1,2-*b*]furan-4,5-diones as novel L-shaped *ortho*-quinone substrates for NAD(P)H:quinone oxidoreductase (NQO1), Eur. J. Med. Chem. 82 (2014) 56–67.

[8] K.K. Karlsen, A. Pasternak, T.B. Jensen, J. Wengel, Pyrene-modified unlocked nucleic acids: synthesis, thermodynamic studies, and fluorescent properties, Chem. Biochem. 13 (2012) 590–601.

[9] F. Hoevelmann, L. Bethge, O. Seitz, Single labeled DNA FIT probes for avoiding false-positive signaling in the detection of DNA/RNA in qPCR or cell media, Chem. Biochem. 13 (2012) 2072–2081.

[10] I.V. Astakhova, T.S. Kumar, J. Wengel, Fluorescent oligonucleotides containing a novel perylene 20 -amino-a-L-LNA monomer: synthesis and analytical potential, Collect. Czech. Chem. C 76 (2011) 1347–1360.

[11] S. Latif, I. Bauer-Sardina, K. Ranade, K.J. Livak, P.Y. Kwok, Fluorescence polarization in homogeneous nucleic acid analysis II: 50 -nuclease assay, Genome Res. 11 (2001) 436–440.

[12] S.A.E. Marras, S. Tyagi, F.R. Kramer, Real-time assays with molecular beacons and other fluorescent nucleic acid hybridization probes, Clin. Chim. Acta 363 (2006) 48e60.

[13] S.U. Hettiarachchi, B. Prasai, R.L. McCarley, Detection and cellular imaging of human cancer enzyme using a turn-on, wavelength-shiftable, self-immolative profluorophore, J. Am. Chem. Soc. 136 (2014) 7575–7578.

[14] W. Zhou, D. Leippe, S. Duellman, M. Sobol, J. Vidugiriene, M. O'Brien, J.W. Shultz, J.J. Kimball, C. DiBernardo, L. Moothart, L. Bernad, J. Cali, D.H. Klaubert, P. Meisenheimer, Self-immolative bioluminogenic quinone luciferins for NAD(P)H assays and reducing capacity-based cell viability assays, Chem. Biochem. 15 (2014) 670–675.

[15] K.A. Nolan, D.J. Timson, I.J. Stratford, R.A. Bryce, In silico identification and biochemical characterization of novel inhibitors of NQO1, Bioorg. Med. Chem. Lett. 11 (2008) 6246–6254.

[16] K.A. Nolan, H. Zhao, P.F. Faulder, A.D. Frenkel, D.J. Timson, D. Siegel, D. Ross, T.R. Burke Jr., I.J. Stratford, R.A. Bryce, J. Med. Chem. 50 (2007) 6316–6325.

[17] J. Bian, X. Qian, B. Deng, X. Xu, X. Guo, Y. Wang, X. Li, H. Sun, Q. You, X. Zhang, Discovery of NAD(P)H:quinone oxidoreductase 1 (NQO1) inhibitors with novel chemical scaffolds by shape-based virtual screening combined with cascade docking, RSC Adv. 5 (2015) 49471–49479.

[18] K.A. Scott, J. Barnes, R.C. Whitehead, I.J. Stratford, K.A. Nolan, Inhibitors of NQO1: identification of compounds more potent than dicoumarol without associated off-target effects, Biochem. Pharmacol. 81 (2011) 355–363.

[19] M. Hassani, W. Cai, K.H. Koelsch, D.C. Holley, A.S. Rose, F. Olang, J.P. Lineswala, W.G. Holloway, J.M. Gerdes, M. Behforouz, H.D. Beall, Lavendamycin antitumor agents: structure-based design, synthesis, and NAD(P)H:quinone oxidoreductase 1 (NQO1) model validation with molecular docking and biological studies, J. Med. Chem. 51 (2008) 3104–3115.

[20] M. Sameiro, T. Goncalves, Fluorescent labeling of biomolecules with organic probes, Chem. Rev. 109 (2009) 190–212.

[21] K.A. Nolan, J.R. Doncaster, M.S. Dunstan, K.A. Scott, A.D. Frenkel, D. Siegel, D. Ross, J. Barnes, C. Levy, D. Leys, R.C. Whitehead, I.J. Stratford, R.A. Bryce, Synthesis and biological evaluation of coumarin-based inhibitors of NAD(P)H: quinone oxidoreductase-1 (NQO1), J. Med. Chem. 52 (2009) 7142–7156.

[22] M. Faig, M.A. Bianchet, S. Winski, R. Hargreaves, C.J. Moody, A.R. Hudnott, L.M. Amzel, Structure-based development of anticancer drugs: complexes of NAD(P)H: quinone oxidoreductase 1 with chemotherapeutic quinones, Structure 9 (2001) 659–667.

[23] M.A. Bianchet, M. Faig, L.M. Amzel, Structure and mechanism of NAD[P]H: quinone acceptor oxidoreductases (NQO), Meth. Enzymol. 382 (2004) 144–174.

[24] J. Kim, S. Felts, L. Llauger, H. He, H. Huezo, N. Rosen, G. Chiosis, Development of a fluorescence polarization assay for the molecular chaperone Hsp90, J. Biomol. Screen 9 (2004) 375–381.